Investigation of the Heating and Cooling of Composite Glass Seals for SOFCs

Honors Thesis

The Ohio State University
Department of Mechanical Engineering

Timothy J. Gatts

The Ohio State University
Columbus, OH, USA
College of Engineering
Department of Mechanical Engineering

Investigation of the Heating and Cooling of Composite Glass Seals for SOFCs

Honors Thesis

Timothy J. Gatts
RD#3 Box 83
Moundsville, WV 26041

Advisor: Dr. Mark Walter, Associate Professor
Department of Mechanical Engineering

May 16, 2008

Acknowledgements

I would like to thank my research advisor, Dr. Mark Walter, for all of his help and support throughout the entire project. I would also like to thank Himanshu Bhatnagar for helping me create the Ansys™ simulation and Dr. Rebecca Dupaix for helping me debug the Ansys™ simulation. Gary Gardner and Neil Gardner in the Mechanical Engineering machine shops helped me greatly in the machining of fixtures used in the experimental setup. I would like to thank Dr. John Lannutti for allowing me to use equipment in his Solid Oxide Fuel Cell Manufacturing and Reliability Laboratory and David Lee for helping me use the test equipment in the lab. Funding for the project in Summer 2007 came from OSU's Office of Technology Enhanced Learning and Research (TELR) via the Digital Union, and the test specimens were provided by NexTech Materials, Ltd.

Abstract

Since the Industrial Revolution in the 19th Century, fossil fuels have been burned to produce power and heat. The inefficiency of the combustion process coupled with a dwindling supply of fossil fuels necessitates the need for new fuel sources and new methods for more efficient energy conversion. Solid Oxide Fuel Cells (SOFCs) are one of many emerging technologies that can help to replace fossil fuel combustion. SOFCs allow for the use of various hydrogen-rich fuels to produce electricity and waste heat. The only byproducts of SOFCs are water, heat, and sometimes carbon dioxide depending on the fuel, which are all safer than carbon monoxide given off in fossil fuel burning. The energy conversion method is much more efficient than fossil fuel combustion, and the byproducts are in general much cleaner and safer for humans and the environment. SOFCs are, however, still in development. One particular challenge for SOFCs is related to the need to isolate or seal the reductant (fuel) on the anode side and oxidant (oxygen) on the cathode side of each individual cell. Since they operate at high temperatures (700°C -1000°C), SOFCs are prone to failure due to thermal expansion mismatches between the various components.

This project involves the investigation of three potential SOFC seal materials. The three seals are composed of 50% glass - 50% Zirconia, 75% glass - 25% Zirconia, and 100% glass. Each seal is used to create an annulus between two disks of Scandium-stabilized Zirconia (ScSZ) which is a ceramic used as an SOFCs electrolyte. The seal materials are also used to form an annulus between an ScSZ disk and a disk of crofer, a chromium-iron alloy commonly used for SOFCs interconnects. The seals are heated from room temperature to a typical SOFC operating temperature, held at operating temperature, and cooled back to room temperature. This temperature profile simulates the start-up, operation, and cool-down of an actual SOFC. The seals are tested for failure by Acoustic Emission (AE) analysis. The AE results are then verified using Finite Element Analysis (FEA) simulations. The experimental results are used to determine when in the thermal cycle seal failure occurs, and the FEA simulations are used to determine the most likely reason for failure and location of failure.

The experimental results show that for all seal materials and all interfaces, significant seal degradation occurs during the cooling of the materials from high operating temperature to room temperature. For sealing ScSZ to ScSZ, the 100% glass seal is found to be the least prone to failure. For sealing ScSZ to crofer, the results are less clear cut. These results are characterized by critical time, t_{cr}, which is defined by the time from the start of cooling until failure. Based on the analysis of t_{cr}, all three seals fail, but 50% glass - 50% Zirconia has the largest t_{cr}. These results indicate that using glass seals with a ceramic reinforcement is where future research should follow. After testing is complete, the seal materials remain attached to the ScSZ disk but have become detached from the crofer disk. Based on these results, the expected mode of failure is separation of the seal from the crofer. The FEA simulation results validate this observation. The stress at the seal/crofer interface is compressive during most of the heating stage. However, during the hold at operating temperature the stress becomes tensile, and during cooling the tensile stress increases. It can be inferred from the data that when the tensile stress reaches some threshold the bond between the glass seal and the ceramic disk will be broken, and the material will separate.

Table of Contents

List of Figures

List of Tables

1. Introduction/Motivation

Fossil fuels have been used as the primary energy source for powering homes, industrial plants, and transportation since the Industrial Revolution of the 19th Century. The burning of fossil fuels has led to widespread air, water, and soil pollution. This, along with the quickly dwindling supply of fossil fuels, creates the need to find new methods of cleaner power production that can utilize alternative fuels.

Assuming that it may be possible to one day obtain hydrogen from electrolysis, fuel cells provide an energy conversion method that could reduce and eventually eliminate the use of fossil fuels. Fuel cells separate electrons from hydrogen or a hydrogen-based fuel, which through an electrical circuit as electrical current. The result is the direct conversion of chemical energy in the fuel to usable electrical energy, with clean water being the only byproduct. In fossil fuel combustion, thermal energy (heat) is used as an intermediate step in the energy conversion. Since thermal energy is less efficient than either chemical or electrical energy, the heat conversion step results in energy being lost to the surroundings. The lack of an intermediate heat step results in fuel cells being much more efficient than fossil fuel combustion [1].

Solid Oxide Fuel Cells (SOFCs) are a type of fuel cell with a very high operating temperature (700-1000°C). Figure 1 shows a diagram of the basic operating principles of an SOFC.

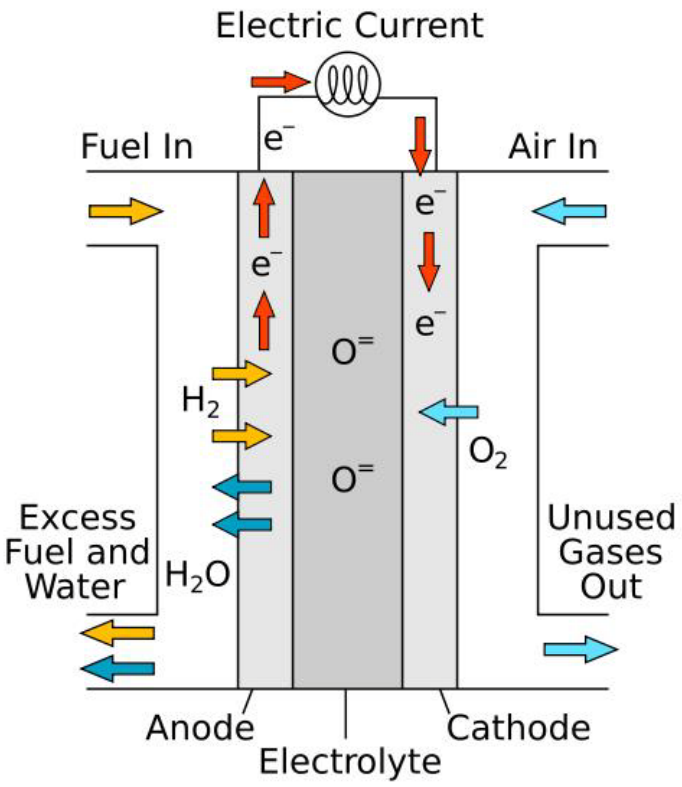

Figure 1: Diagram of the operation of an SOFC [2]

The high operating temperatures give a few advantages for SOFCs over other types of fuel cells such as Proton Exchange Membrane (PEM) Fuel Cells and Phosphoric Acid Fuel Cells (PAFC). The main advantage is that SOFCs can utilize a variety of hydrogen-based fuels, whereas some other types of fuel cells require pure hydrogen. Since pure hydrogen does not occur naturally, the burning of fossil fuels is generally required to separate hydrogen from other sources. This, in effect, makes fuel cells that require pure hydrogen fuel less efficient than SOFCs once hydrogen production is taken into account. Because of their high operating temperatures, SOFCs can utilize various hydrogen-based fuels that contain impurities that 'contaminate' other fuel cell types with lower operating temperatures. Another advantage of operating at high temperatures is that SOFCs can be used in 'cogeneration' with steam turbines, where the heat given off by SOFCs are used in combination with the burning of fossil fuels in the steam generation process [3]. Additionally, SOFCs used as a stand-alone electricity source for a building can be used as a heat source for the same building during cold seasons.

The high operating temperatures that give SOFCs advantages over other fuel cell types also cause some problems. Because of mismatches in thermal expansion between metal and ceramic SOFC components, seal degradation can occur at the interfaces during heating at start-up and cooling at shutdown. The ceramic and metal components are necessary to the operation of SOFCs because of their chemical, mechanical, and electrical conductivity properties. Therefore, the only option is to find a viable sealing material. The seal must prevent fuel and air from leaking, and it must remain intact during heating and cooling between room temperature and operating temperature. This problem is explained in further detail in Section 2. The purpose of this research is to test the interface integrity of three different SOFC seal material options through an entire cycle of heating to 815°C, holding at 815°C for a predetermined period, and cooling back to 23°C. The viability of each of these seal materials will be analyzed based on the experimental results.

This report further details SOFC seal failure. Acoustic Emission (AE), Finite Element Analysis (FEA), and glass characterization, which are all used in the testing and analysis of seal materials, are also explained. The experimental procedures and data analysis techniques are described in detail. The results of the analysis and conclusions based on the results are also included.

2. Project Background

2.1 Solid Oxide Fuel Cell (SOFC) Seal Failure

The high operating temperatures that give SOFCs many of their advantages also cause some problems that are preventing the SOFCs from becoming commercially viable. SOFCs are generally used in a stack, which is a group of SOFCs attached together to give a greater overall power output. There are two types of SOFC stacks: tubular and planar. The planar SOFC stack is desirable because it has good cost efficiency and higher power density [4]. A typical SOFC stack is shown in Figure 2.

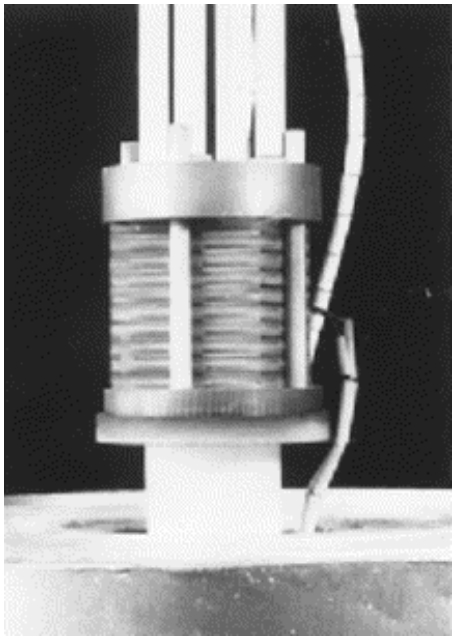

Figure 2: A ten-cell planar SOFC stack before operation [5]

The main concern with using planar stack designs rather than the tubular designs is that planar stack designs requires more extensive use of seals between the edges of the electrodes, electrolytes, and interconnects [5]. A schematic of a planar stack SOFC with the seal locations highlighted is shown in Figure 3.

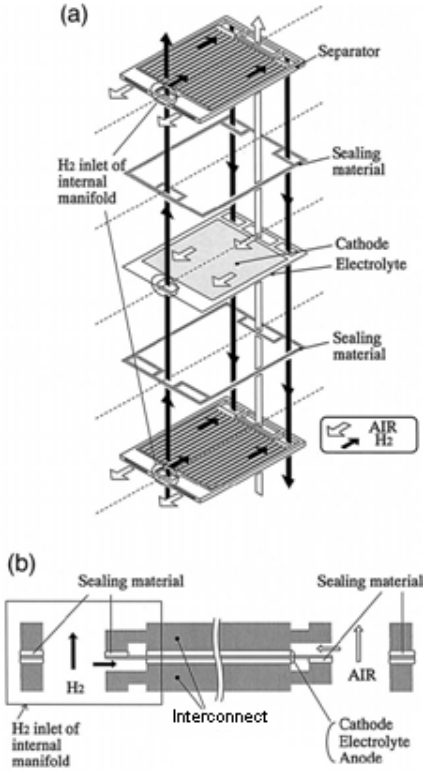

Figure 3: SOFC planar stack model [1]

These seals must keep fuel and oxidation gases separate [6]. There are many requirements a material must meet to qualify as a reliable seal material. Intermediate temperature SOFCs operate at temperatures around 850°C, and the seal must be structurally and chemically stable at this temperature and below [5]. Also, the coefficient of thermal expansion of the seal material must be near that of the other parts of the SOFC to avoid failure caused by thermal mismatch stresses [5]. Since this is typically not possible given the dissimilar materials used for electrodes, electrolytes, and interconnects, seals will ideally have some compliance. The need for compliance is offset by the need for strong bonding that forms a tight seal. Seals are required to remain leak-proof for the entire life of a SOFC, which is upwards of 50,000 hours of operation [5]. Ideally seals would also be able to tolerate both foreseen and unforeseen shutdown and startup events. For expected startup and shutdown the heating and cooling rates are carefully controlled to avoid damage. Typical heating and cooling rates are 2 °C/min and 3 °C/min, respectively. The fast cooling rates associated with unexpected shutdown can cause significant damage because of stresses resulting from thermal gradients.

Over the last ten years, researchers have tried to develop non-degrading seals that can prevent fuel leakage. The earliest seal material tested for use in SOFCs was glass [1]. However, the contact areas between the glass and the electrodes caused failure of the material. To prevent seal fracture, researchers tried reinforcing the glass seals with ceramic fibers [7]. The ceramic-reinforced seals were more durable than the glass only seals, but were more prone to slow leaking. The ceramic-reinforced seals were more durable than the glass only seals, but were more prone to slow leaking. A recent alternate approach to seal design has been the incorporation of platy powders, such as mica and talc. These powders are tape cast to form a gasket that is then mechanically compressed during operation. In ongoing work, this approach has been used to seal laboratory-scale fuel cells [8-14]. The research presented here is conducted on seals that are composed of glass and glass-ceramic composites.

2.2 Acoustic Emission (AE)

Acoustic Emission (AE) analysis is a method of material testing that is used to detect fractures and other material failure. When a material fractures or deforms at the microstructural level, energy is released and mechanical waves are emitted. These mechanical waves travel throughout the material and can be detected by piezoelectric sensors coupled to specimen surfaces. The sensor then relays the wave signal to a data acquisition computer. Figure 4 shows a small example of a sensor output that could be obtained from AE analysis.

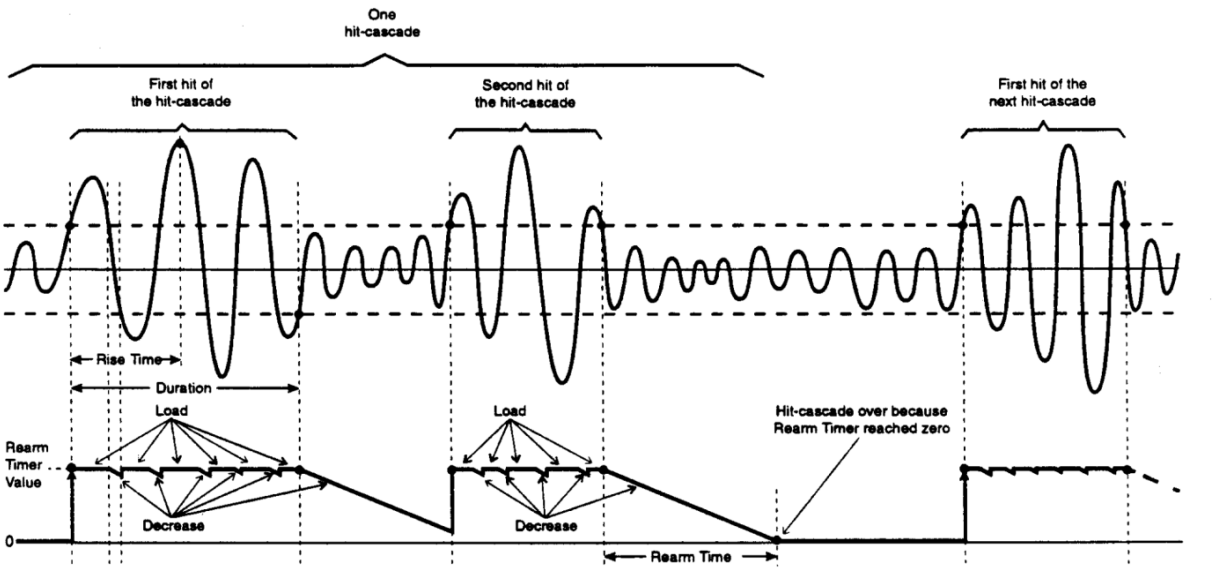

Figure 4: Example AE wave describing data acquisition for AE analysis [15]

As seen in Figure 4, the AE piezosensor is constantly providing output. Therefore, a threshold (shown by the two dashed lines in the figure) must be chosen to determine which portions of the wave are caused by material failure events and which are 'normal.' Once the threshold is crossed by the wave, a 'hit' and a 'hit-cascade' (sometimes called 'events') begin. The hit continues for as long as the wave peaks are outside of the threshold. Once a hit ends, a rearm timer (usually about 2 μs) begins to count down. If the wave crosses the threshold again before the rearm timer reaches zero, a second hit begins as part of the same hit-cascade. However, if the rearm timer reaches zero, then a new hit-cascade begins the next time the threshold is crossed. Figure 4 shows three hits during the time span shown. The first two hits are part of one hit-cascade, while the third hit is the start of another hit-cascade.

There are many ways that AE software can describe an AE wave without storing the entire waveform. Continuous data acquisition is difficult to obtain with the complete wave and would require large amounts of hard drive space. Every event and hit is stored in its own line of a data file along with the additional information describing the event including amplitude, energy, number of hits, and counts. These different aspects of the AE wave can be used to quantify how 'large' an AE event is, which in turn can help quantify the extent of material damaged that has occurred. The amplitude is the height of the highest peak of the wave in decibels recorded during the event. The energy is found by integrating the root-mean-square of the wave during the event. The analysis software uses generic energy units. Therefore, the energy can be used to compare events to each other, but otherwise it has no meaning in terms of the standard use of energy in engineering terms. The number of hits is the total number of hits recorded during an event. A count, on the other hand, is the total number of peaks that cross the threshold during a specific event. The count can be equal to the number of hits for an event if each hit contains only one peak above the threshold, but it is often greater than the number of hits. The count can never be less than the number of hits for an event. In this research, all four aspects of the AE wave

have been analyzed, but all lead to the same conclusions. Therefore, this work will present only the number of counts to characterize seal performance.

2.3 Finite Element Analysis (FEA)

Finite Element Analysis (FEA) is a numerical method of solving complex engineering problems that cannot be analytically solved otherwise. In FEA structures, thermal bodies, etc. are discretized into finite elements called nodes. The most basic FEA models, such as simple springs and beams, can be solved by simple matrix mathematics. In these problems, each node represents a spring junction or beam section. In these cases, the problem is fully defined by FEA. The idea of using matrices to solve simple engineering problems can be expanded to solve a variety of more difficult problems involving complex geometries, multiple materials, complex material models, etc. In complex problems, the nodes represent a discrete part of the entire structure. In theory, every object is made up of infinitely many nodes. FEA models an object as a finite set of these infinite nodes. Using more nodes to model the structure will yield more accurate results, but solving the problem becomes more difficult. Using fewer nodes makes the problem simpler to solve, but it makes the nodes less representative of the structure as a whole. Therefore, there is a trade-off between the complexity of the problem and the accuracy of the results.

For complex problems, an FEA program, such as Ansys™, is used to numerically solve the problem. FEA problems can be solved by computers with many more nodes in much less time than by hand calculations. This allows for faster, more accurate results. However, there is a limit to both accuracy and speed in solving problems with FEA even with the use of a computer.

In FEA computer programs, areas are 'meshed' into discrete elements of much smaller size. Each intersection between elements is a node. Finer meshes refer to the use of smaller elements and more nodes. The finer the mesh is made, the more accurate the final results are. However, using meshes that are too fine are time consuming even for computers. Therefore, finding an optimal mesh size is significant in solving FEA problems in Ansys™. The most common method for determining optimal mesh size is to begin with a coarse mesh. Multiple simulations are run, refining the mesh after each simulation. The mesh is considered optimal when the results converge within an acceptable accuracy compared to the previous mesh (usually less than 5% difference). Once the results have converged, the results are recorded. This method prevents the use of too fine meshes from the onset that can lead to time consuming simulations.

2.4 Glass Characterization

Before FEA can be utilized, material properties for all of the materials in the model must be known. The main properties needed for the current simulations are modulus of elasticity, Poisson's ratio, and coefficient of thermal expansion. These properties are known for crofer and can be estimated for Scandium-stabilized Zirconia by using other comparable ceramics. However, the properties of the glass composite seals are unknown. When glass is exposed to high temperatures it can creep; therefore creep properties will be needed for accurate modeling. Creep models for glass are not readily available,

so tests must be performed on glass to get a good material model for FEA. Therefore, material testing is necessary to get all of the necessary properties for glass.

3. Experimental Setup

3.1 Test Specimens

A total of 6 test specimens are used in the AE testing of SOFC seals. Three specimens consist of ceramic (Scandium-stabilized Zirconia) to ceramic; the other three specimens consist of ceramic sealed to metal (crofer, a chromium-iron). Each of the three ceramic-ceramic specimens and three ceramic-crofer specimens are sealed together using one of three different composites of glass and Zirconia: 50% glass/50% Zirconia, 75% glass/25% Zirconia, and 100% glass.

The specimens are circular with 1.5” diameter. The seal material is sandwiched between the two materials being sealed together, and it extends inward from the edge of the specimen; all but the center 0.5” is sealed together. Figures 5-6 show the specimens separated into two disks. Figure 5 is the crofer disc. Figure 6 is the Scandium-stabilized Zirconia (ScSZ) disc with the sealing material still attached.

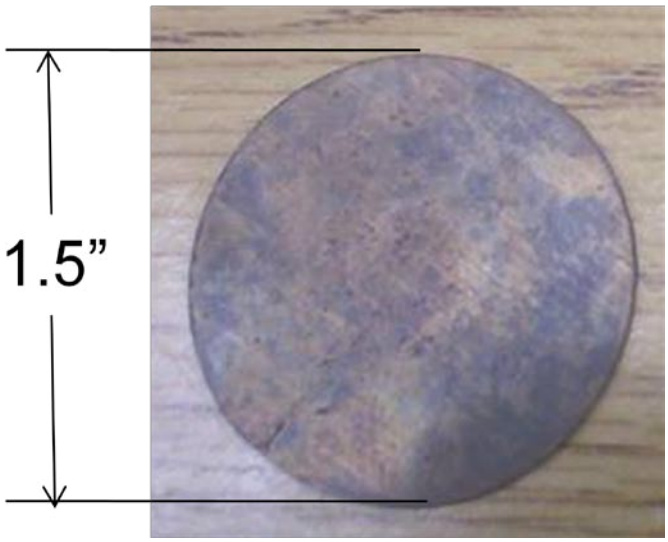

Figure 5: Crofer disk taken from one of the test specimens

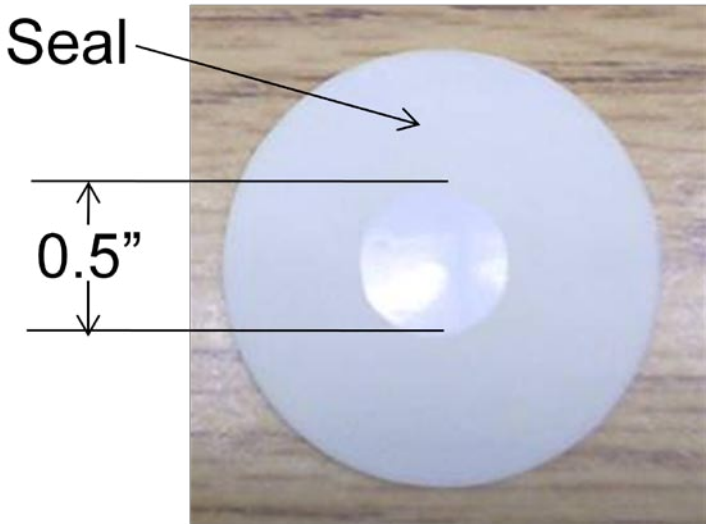

Figure 6: Scandium-stabilized Zirconia disk with glass seal still attached

3.2 Heating/Cooling Cycle

The heating/cooling cycle used for testing SOFC seals consists of three stages: heating to typical SOFC operating temperature, holding at operating temperature, and cooling back to room temperature. The heating begins at a rate of 2°C/min until the specimen reaches 450°C. Heating continues to 815°C at a rate of 3°C/min. The entire heating portion of the cycle lasts between 6-7 hours before operating temperature is reached. The heating stage of the heating/cooling cycle during AE testing simulates the startup of an SOFC.

The holding stage of the cycle begins once the temperature reaches 815°C. The specimen is held at this temperature for 60 minutes. Although a normal SOFC operates at high temperatures for periods of multiple days/weeks, it has been determined that 60 minutes is long enough for the materials to reach steady-state and stop expanding/shifting.

The cooling stage, like the heating stage, consists of 2 parts. First, the specimen is cooled to 500°C at a rate of 3°C/min. Once the temperature reaches 500°C, however, the natural cooling of the furnace becomes too slow to control. Since the furnace has no cooling capability, the specimen is allowed to cool at the slowing natural cooling rate. Because of this, the cooling stage takes about 12 hours to reach room temperature.

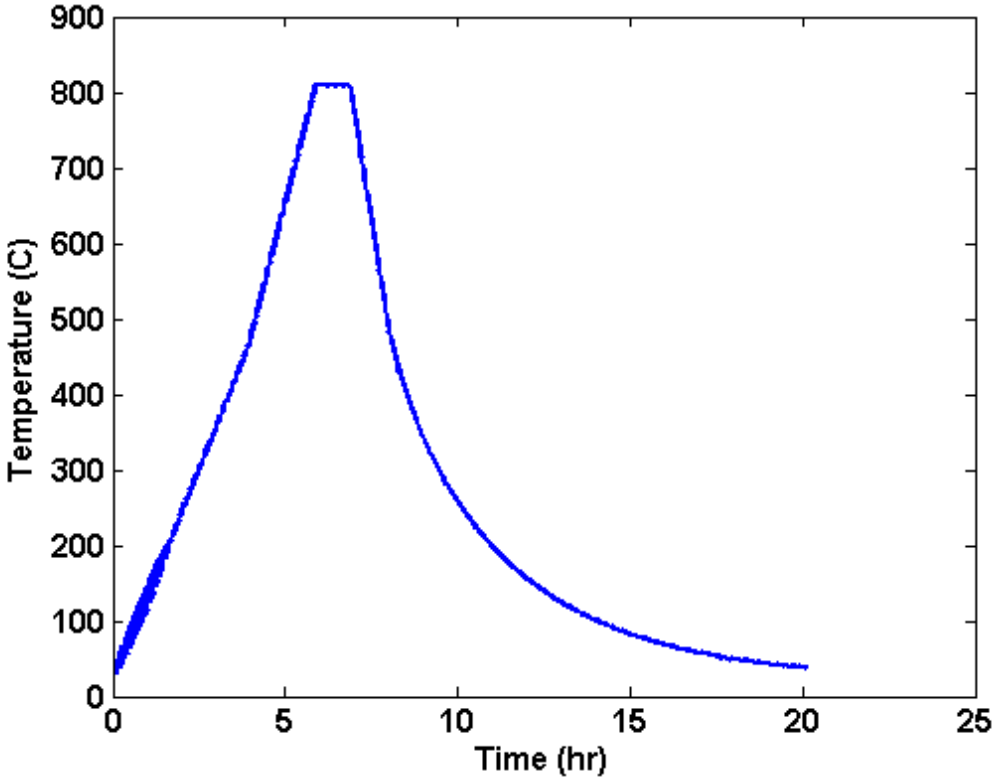

Figure 7: Heating/cooling cycle used for AE testing of SOFC seals

The temperature of the furnace is controlled by an Applied Test Systems PID controller. The controller is programmed through a system of step and hold functions to give the desired temperature profile inside the furnace. The heating portion of the cycle is composed of a 2°C/min ramp function and a 3°C/min ramp function. A hold function keeps the temperature constant for one hour. Next, another ramp function allows the furnace to cool at 2°C/min. Finally, a stop function shuts down the furnace to allow for cooling to room temperature.

3.3 AE Testing

For the AE analysis, the specimen "floats" in a high temperature box furnace between two alumina rods that act as wave guides. The alumina rods allow for the AE wave to propagate to the sensors, while allowing the sensors to remain safely outside the furnace. Each alumina rod is connected to a piezoelectric AE sensor that is held in place by a metal bracket and nylon bolt as seen in Figure 8. The AE data from the sensors and temperature data from a thermocouple is compiled by a Vallen-Systeme AE workstation with analysis software. A schematic of the AE setup is shown in Figure 8.

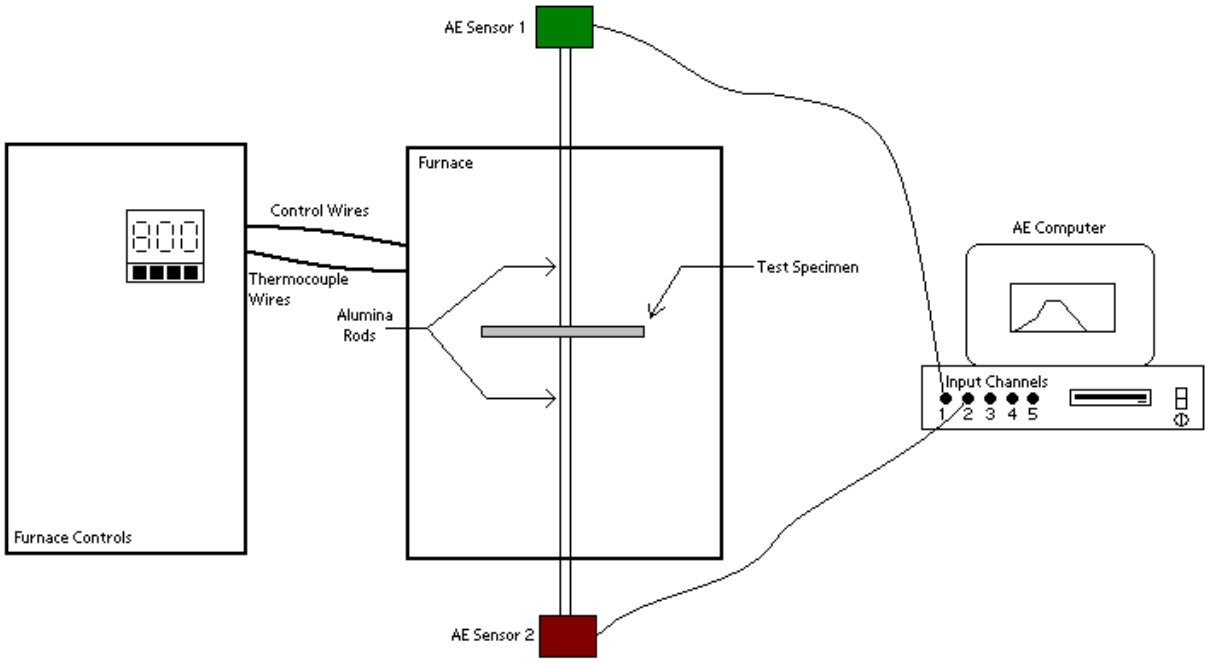

Figure 8: Schematic of the AE test setup

As seen in the figure, one alumina waveguide contacts the bottom of the specimen and one contacts the top. Since the alumina rods are of equal length, events that come from the specimen should be recorded by the AE system at very nearly the same times. The use of two sensors acts as a filter that separates events caused by material failure from events caused by external noise, including electrical noise and vibrations in the laboratory. Events that appear either in only one channel or with a significant time delay are assumed to originate outside the specimen. Data filtering can then be accomplished using a Matlab script file that sorts out all events picked up by both sensors at the same time. Figure 9 shows data taken from AE analysis before and after the Matlab filter is applied. The 79% reduction in events shows how vital the filter is for obtaining good data.

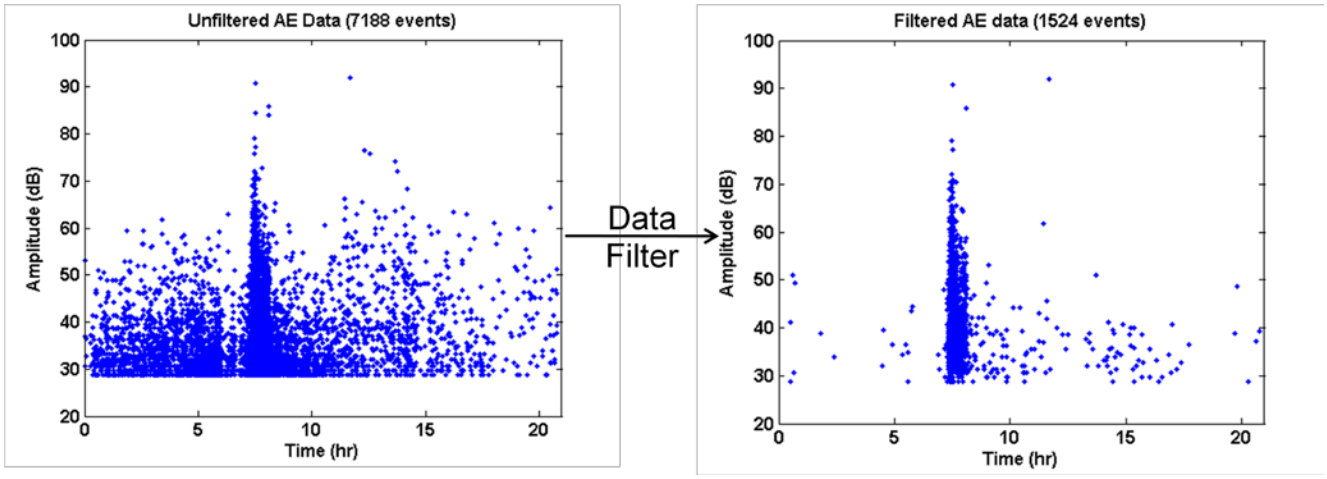

Figure 9: AE data from before and after the Matlab filter is applied

Figures 10-12 are images of the actual AE setup. Figure 10 shows a photograph of the furnace with a test specimen being placed inside. One alumina rod and AE sensor can be seen coming out of the top of the furnace. Figure 11 is a photograph of an AE sensor being clamped in a sensor bracket. The epoxy interface between the sensor bracket and the alumina rod can also be seen. Figure 12 is a photograph of the data acquisition computer with the AE software open and running on the screen.

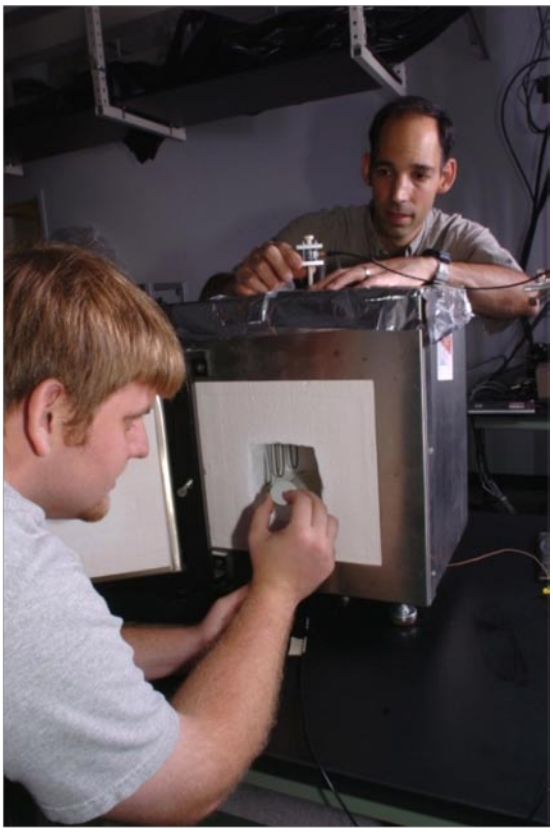

Figure 10: Photograph of the furnace with test specimen, alumina rod, and AE sensor

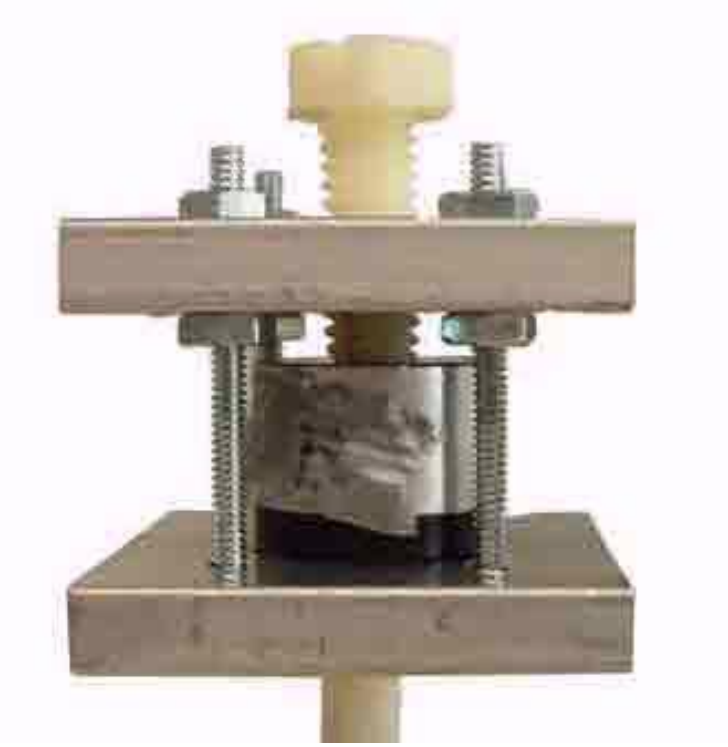

Figure 11: Enlarged photograph of AE sensor clamped in place be sensor bracket

Figure 12: Data acquisition computer with AE software running

3.4 Material Testing for Glass Characterization

Corning 7740 glass is used for obtaining typical glass properties as a function of temperature. The specimens are cylindrical with 8 mm diameter and 16 mm length, resulting in a 2:1 length to diameter ratio as specified by ASTM E139. Two types of room temperature and high temperature compression tests are performed on the glass specimens: stress/strain tests and creep tests. Experiments are performed on a Test Resources 1000R12 load frame with Test Resources 3210 split-oven furnace.

The stress/strain tests are performed by loading the specimen at constant displacement until 400 lb of force is reached. The specimen is placed on the load frame, and the furnace is locked in place around the specimen. The furnace is then heated to the desired temperature. The two temperatures used for this glass characterization are 200°C and 350°C. Once the specimen and load frame have reached equilibrium after one hour, the loading of the specimen begins. The load frame displaces at a rate of 0.0001 inches/second. The loading continues for about one minute until the load reaches 400 lb. The strain is measured by a high temperature extensometer (Epsilon Model 3448-0100-010) connected to the load frame. Load is measured by a 1000 lb force transducer.

The creep tests are performed by compressing the specimen to a specified load and holding the load constant at a given temperature. The specimen is placed on the load frame, and the furnace is locked in place around the specimen. The furnace is then heated to the desired temperature. The two temperatures used for this glass characterization are 200°C and 500°C. Once the furnace reaches the desired temperature, the specimen and load frame are left for one hour to allow everything to reach equilibrium at the elevated temperature. The load frame then quickly compresses the specimen to the desired load, which is 35 lb for these tests. The specimen remains in compression for at least two hours to allow for adequate strain values to be acquired. The strain is recorded by an extensometer, which is attached to the load frame near the specimen. The load is recorded by a 50 lb force transducer located on the load frame. The data is transferred to a text file for analysis in Matlab.

3.5 FEA Modeling

The FEA simulation consists of an axisymmetric model created in Ansys™, which has very similar dimensions to the specimens used in experiments described above. The model is shown in the Figure 13.

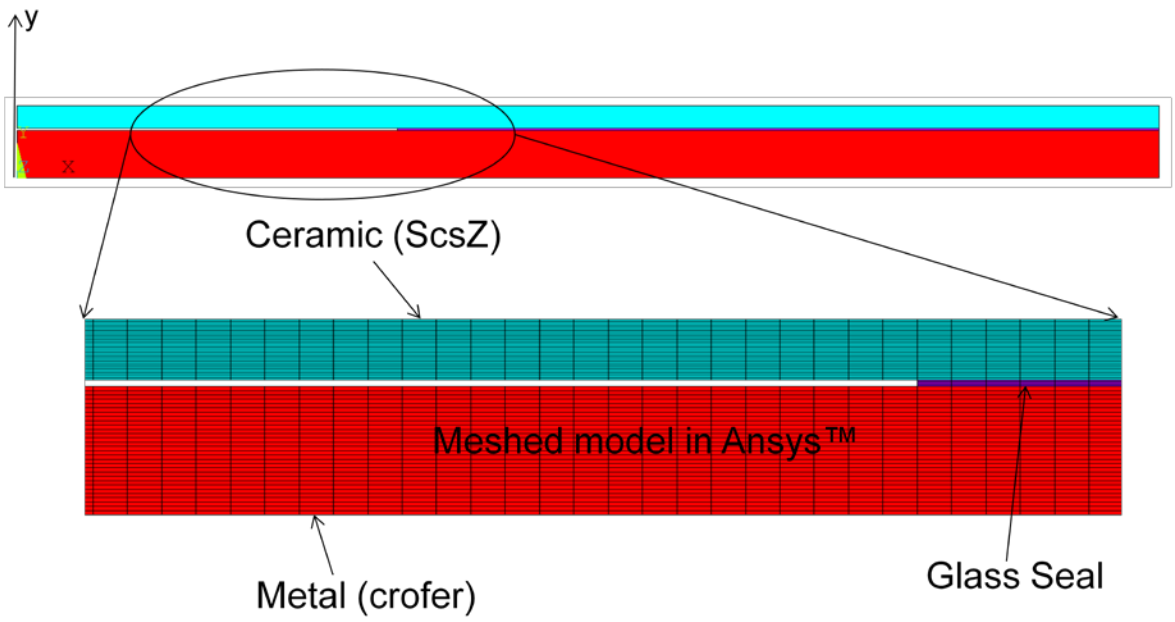

Figure 13: FEA model of seals tested in AE analysis

Applying axisymmetry about the y-axis means that the model represents the seal constructs described above. The Scandium-stabilized Zirconia disk is the blue portion at the top of the model. The glass-Zirconia composite seal is the purple section in the middle of the model. The crofer disk is red area at the bottom of the model. The mesh shown in the figure is done manually to ensure that the nodes at the material interfaces are shared by both materials.

The axes are defined in three dimensions for characterizing stress directions. The x-axis describes the radial direction from the center of the disk. The y-axis describes the direction normal to the surface of the disk. The z-axis describes the direction tangential to the disk.

The three materials each have their own material model for the FEA simulation. The crofer material model is based on material properties found in the literature [16]. The ScSZ material model is based on assumptions using other ceramic material properties. The glass-Zirconia composite seal material model is based on the results of the glass characterization tests. Each material model contains Young's Modulus, E; Thermal Coefficient of Expansion, α; and Poisson's Ratio, ν. The material properties are given in Table 1.

Table 1: Material models used for FEA simulation

Material	E (GPa)	α (/°C)	ν
Crofer	220	$2.912 \cdot 10^{-9} \cdot T$	0.3
100% Glass Seal	90@23°C, 100@350°C	$3.8 \cdot 10^{-6}$	0.23
ScSZ	200	$1 \cdot 10^{-5}$	0.3

The glass-Zirconia composite seal also has an additional creep model for time dependent deformation. The time hardening creep model is used in the FEA simulation [17]. The creep model is:

$$\frac{d\varepsilon}{dt} = c_1 \sigma^{c_2} t^{c_3} e^{-c_4/T} \qquad (1)$$

From the glass characterization tests, the creep constants in Equation 1 are as given in Table 2.

Table 2: Creep constants used in glass-Zirconia seal material model for FEA simulation

c1	$3.8 \cdot 10^{-12}$
c2	1.1
c3	-0.83
c4	100

The temperature profile used in the FEA model is a simplified version of the temperature profile used in the experiments. The first step in the FEA temperature profile is a ramp with constant slope from 0°C to 850°C over a span of 21200 seconds (5.9 hours). The second step in the FEA temperature profile holds the temperature constant for 3600 seconds (1 hour). The third and final step in the FEA temperature profile is a ramp with constant slope from 850°C to 550°C over a span of 11500 seconds (3.2 hours). The profile was simplified in this manner, because the FEA model would require too many load steps to exactly represent the temperature profile in the experiments.

4. Experimental Results

4.1 AE Analysis Results

4.1.1 Ceramic on Ceramic Results

For all three seal materials tested, the ceramic on ceramic specimens had little AE activity over the entire 20+ hour test period. This is not unexpected as the two ceramic disks being sealed together expand and contract at the same rate for changing temperatures. Figures 14-16 show the cumulative results of the AE analysis over the entire time of the test. The figures show the results from the 50% glass - 50% Zirconia seal, the 75% glass - 25% Zirconia seal, and the 100% glass seal respectively. The cumulative hit count is dashed while the temperature profile overlay is solid.

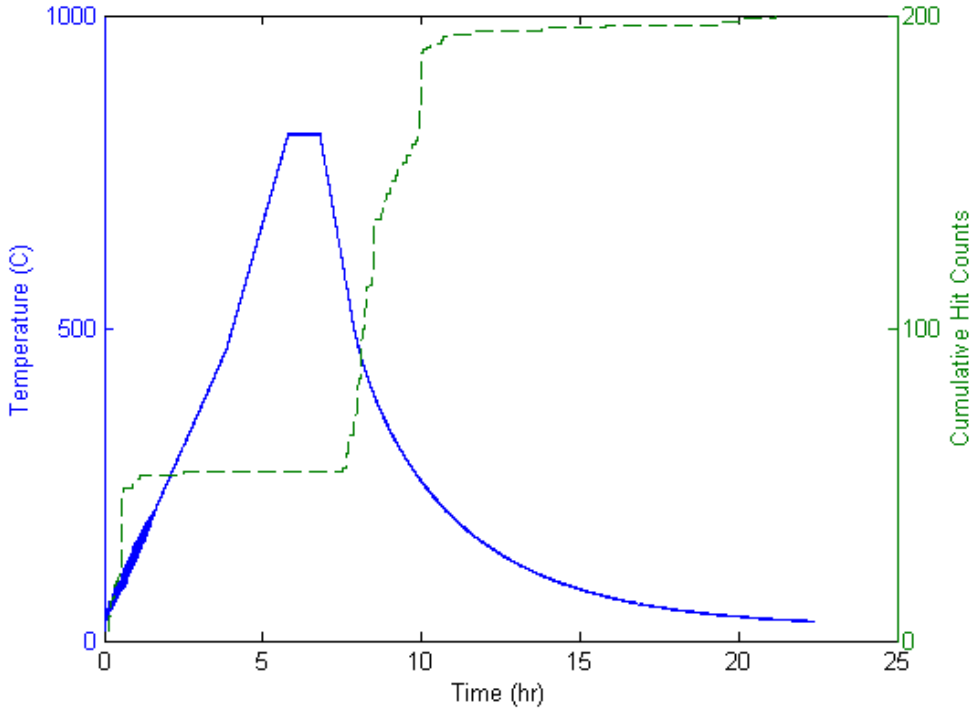

Figure 14: Cumulative hit counts for 50% glass - 50% Zirconia seal ceramic on ceramic

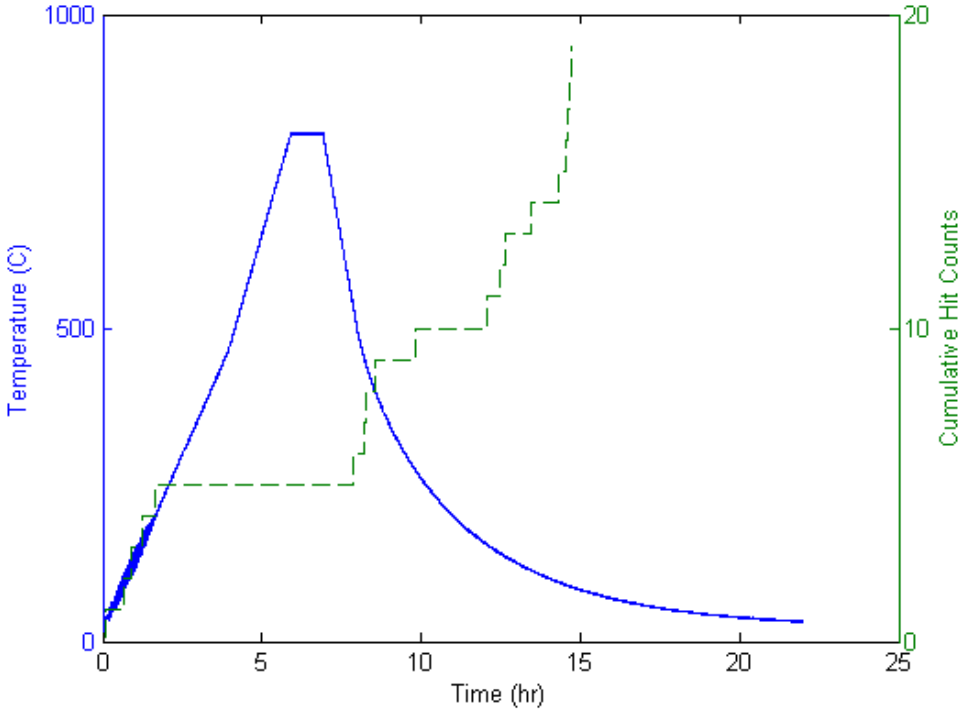

Figure 15: Cumulative hit counts for 75% glass - 25% Zirconia seal ceramic on ceramic

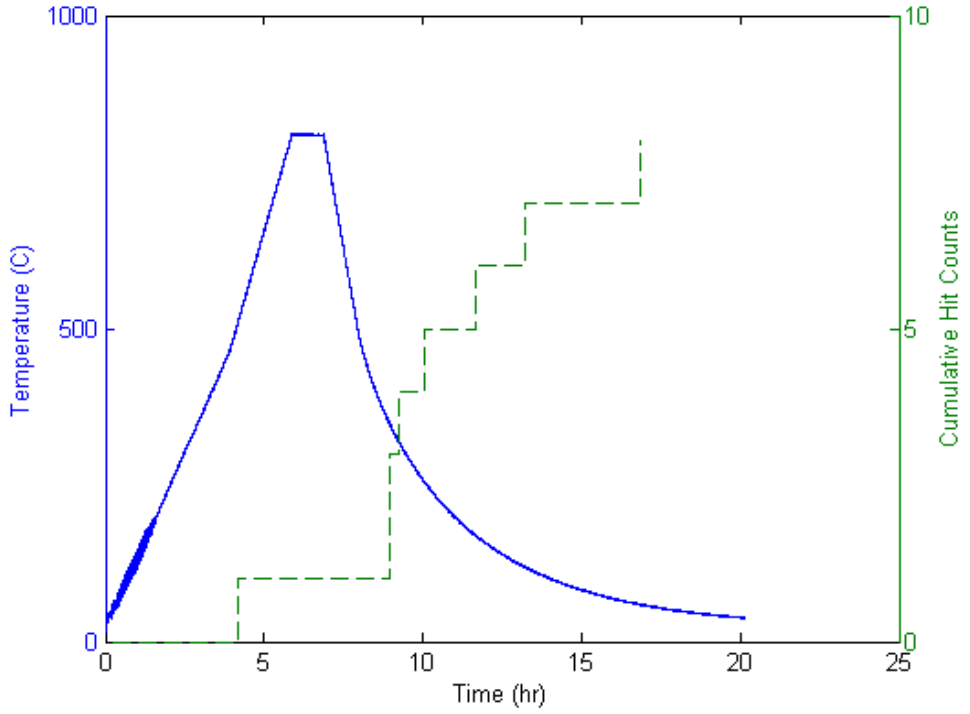

Figure 16: Cumulative hit counts for 100% glass seal ceramic on ceramic

The small amount of AE activity makes an analysis of the AE data difficult to make. However, the 100% glass seal is assumed to be best for sealing ceramic to ceramic, because it has the fewest number of events over the entire testing period (7 AE events in 20 hours). For all tests, some activity occurs during heating, but most occurs during cooling. None of the tests have any activity during the holding stage, which is expected since thermal expansion during temperature changes is the expected cause of failure. In addition, during the hold time, the glass component in the seals has time to relax through creep processes.

4.1.2 Ceramic on Metal Results

The ceramic on metal specimens exhibit much more AE activity than the ceramic on ceramic specimens. The fewest number of events for a ceramic on metal test is over 1000, whereas the greatest number of events for a ceramic on ceramic test is about 200. Because of the total number of events is so large, the total number of events over the testing period may not be a good measure of performance. Therefore, the cumulative hit counts have been normalized so that the end value of the cumulative hit count for each test specimen is 1. The results are shown in Figures 17-20. Figures 17-19 are the results for each individual seal material as in the ceramic on ceramic results. The cumulative hit count is a dashed line while the temperature profile overlay is a solid line. Figure 20 is a zoomed in view of the normalized results for all three seals between 6 hours and 9 hours into the tests.

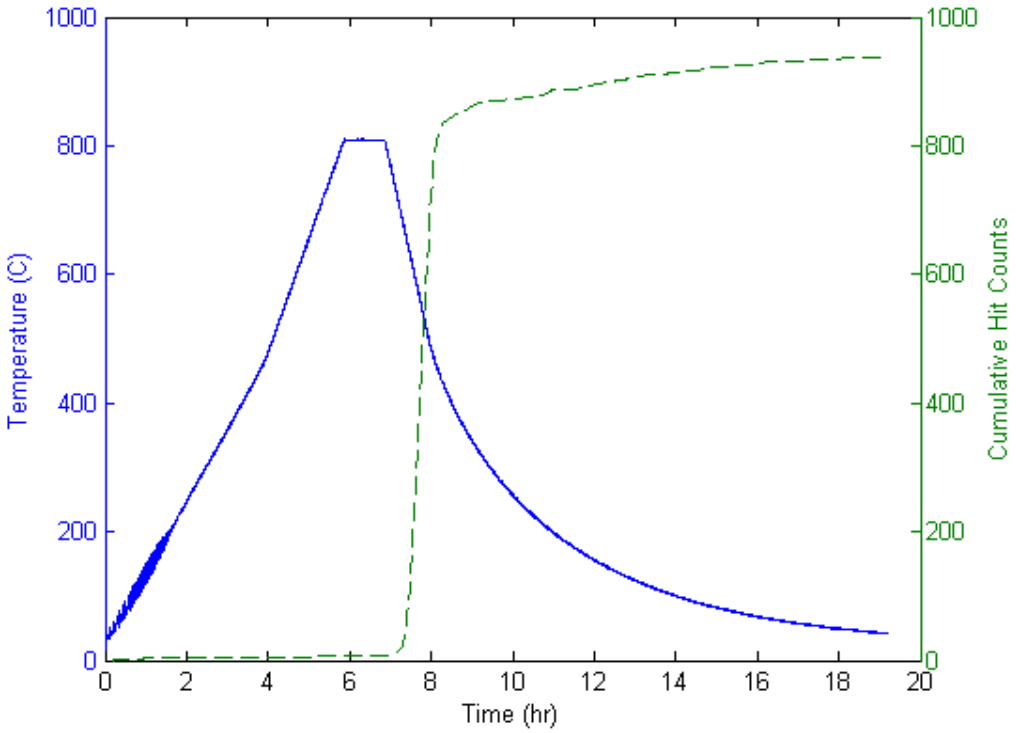

Figure 17: Cumulative hit counts for 50% glass - 50% Zirconia seal ceramic on metal

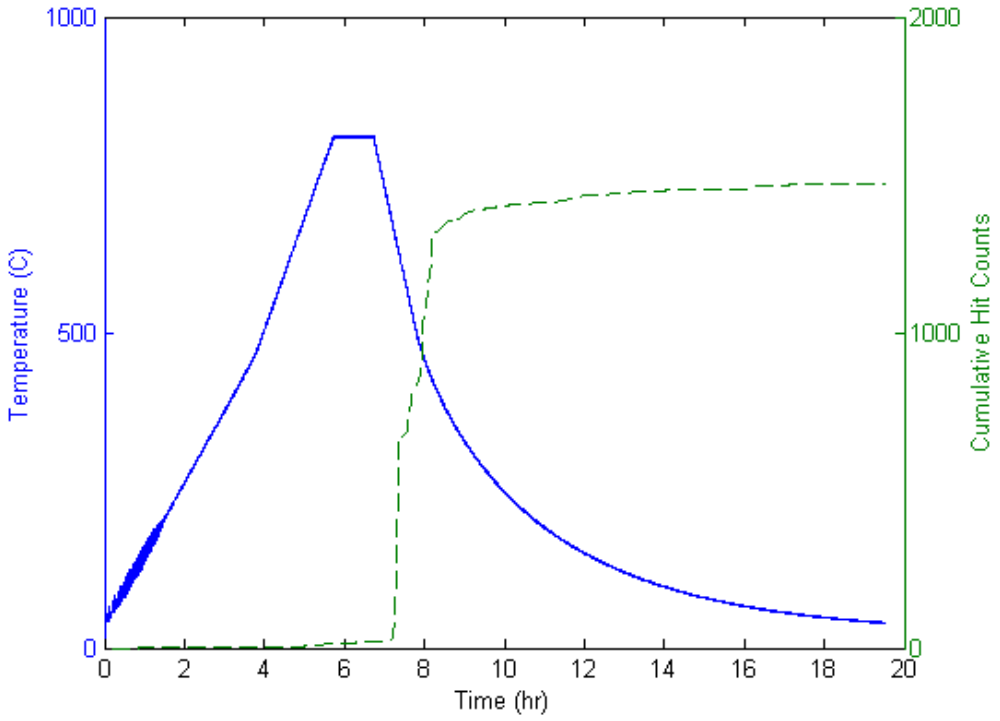

Figure 18: Cumulative hit counts for 75% glass - 25% Zirconia seal ceramic on metal

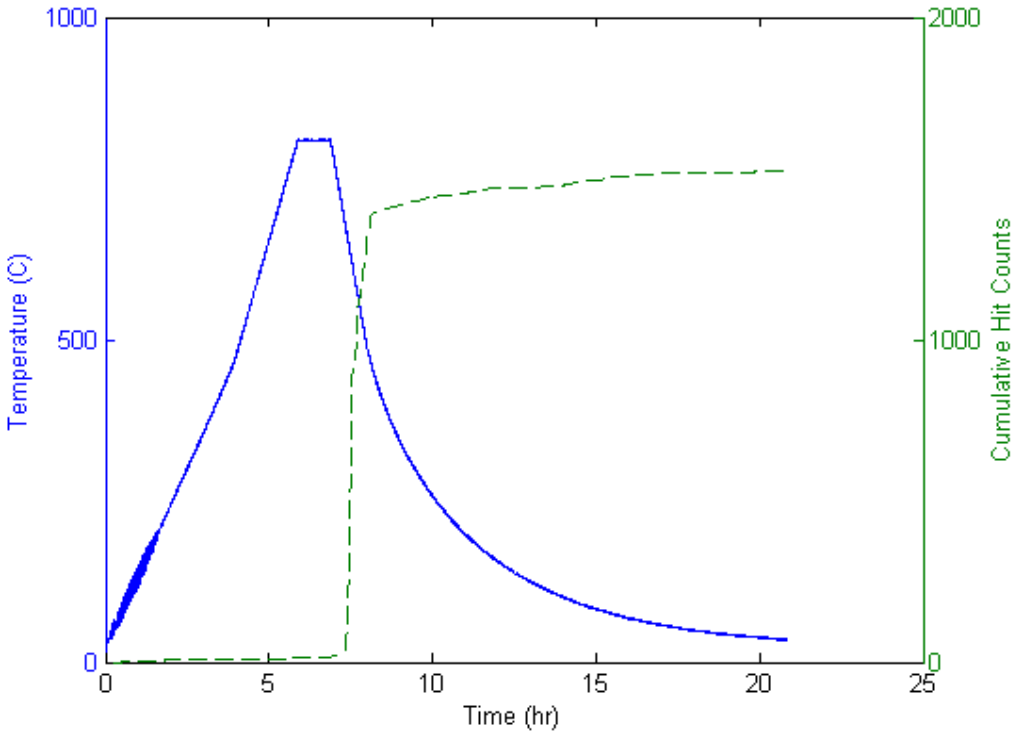

Figure 19: Cumulative hit counts for 100% glass seal ceramic on metal

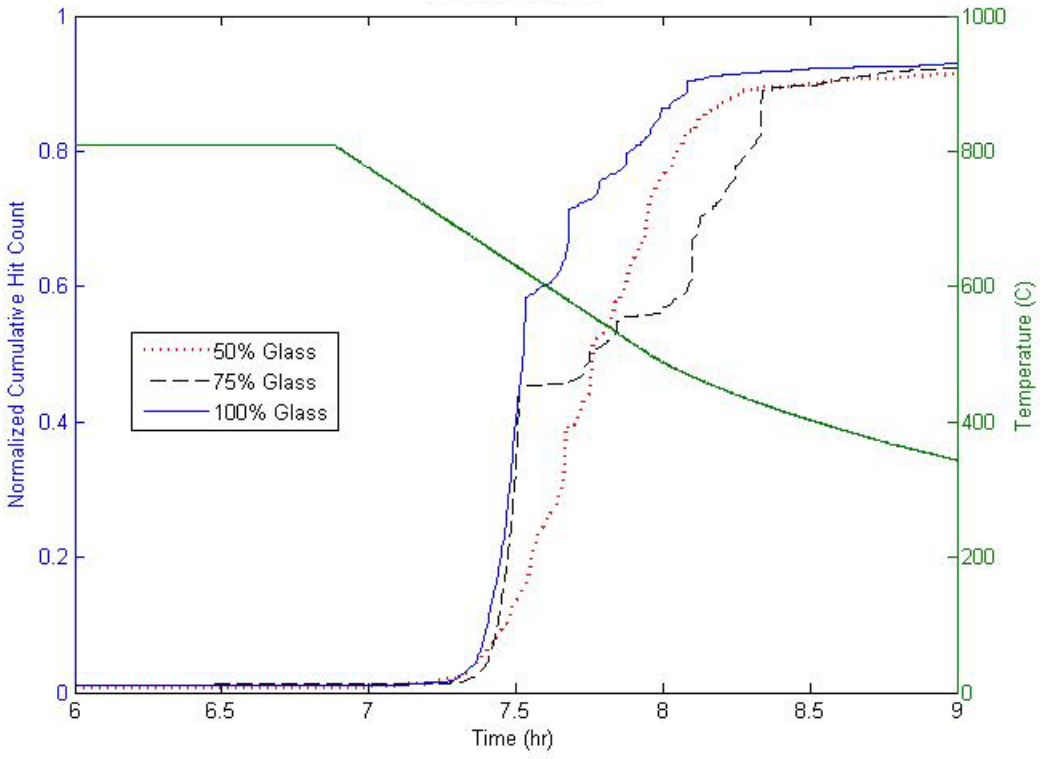

Figure 20: Normalized cumulative hit counts for all seals ceramic on metal

Based on the results shown in the Figures 17-20, most of the seal failure events occur during the beginning stages of cooling. This occurs because of the different rates of contraction of the materials during cooling. The materials expand at different rates during heating as well, but at the high temperatures the glass in the seals begins to soften. However, during cooling the glass in the seals hardens, which makes the seal more likely to fail during cooling than during heating.

The seal performance for the ceramic on metal specimens is characterized by critical time, t_{cr}, the time between the start of cooling and a point when a pre-determined percentage of AE events have occurred. The pre-determined percentage of AE events could be thought of as defining the failure of the seal. Figure 21 depicts how t_{cr} is found for 5% of all AE events for the 50% glass - 50% Zirconia seal.

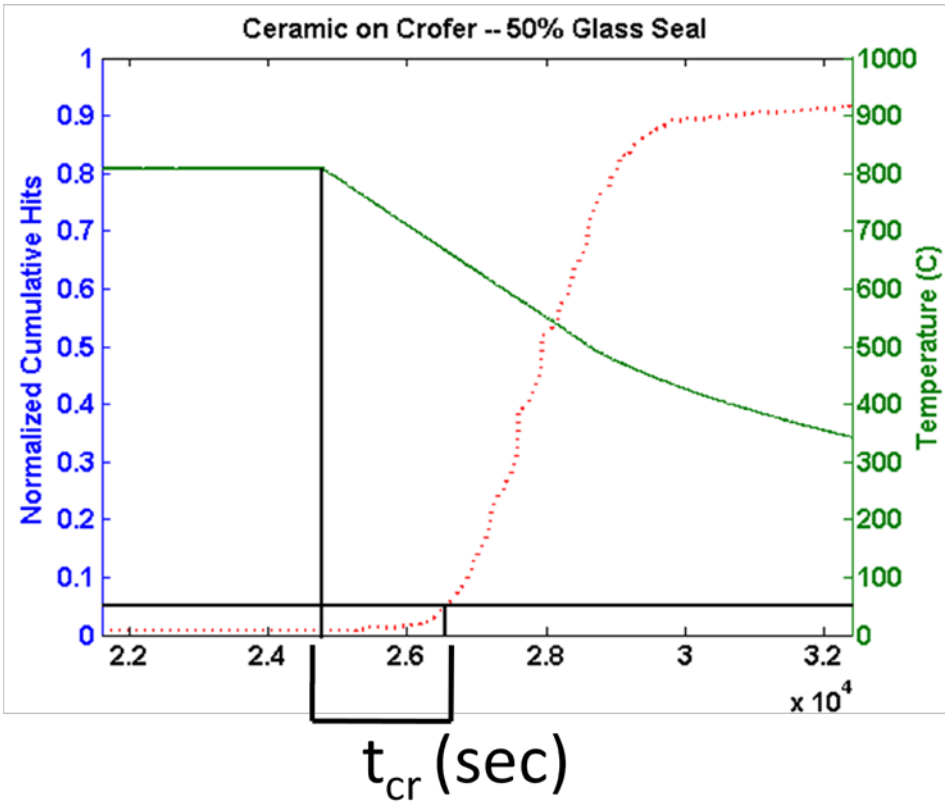

Figure 21: Calculation of t_{cr} for 5% of AE events for 50% glass - 50% Zirconia seal

The range from 5% to 50% is evaluated in increments of 5% for possible values of t_{cr}. These values are shown in Table 3 for each of the three test specimens.

Table 3: Possible values of t_{cr} for all three seal compositions ceramic on metal

	50% Glass	75% Glass	100% Glass
5%	1770	1870	1730
10%	2070	1970	1860
15%	2280	2040	1940
20%	2400	2090	2020
25%	2570	2140	2080
30%	2760	2180	2120
35%	2800	2200	2160
40%	2930	2220	2200
45%	3110	2240	2240
50%	3140	3110	2290

In the table, it can be observed that 50% glass has the largest t_{cr} and 100% has the smallest t_{cr} for every percentage of AE events except for 5%. Therefore, 10% of AE events was chosen for the basis of t_{cr}. The values of t_{cr} are shown in Table 4 for all three seal compositions.

Table 4: Values of t_{cr} for all three seal compositions ceramic on metal

Seal	50% Glass	75% Glass	100% Glass
t_{cr}	2070 sec	1970 sec	1860 sec

Based on the values of t_{cr}, the 100% glass seal fails first and the 50% glass seal fails last. The 50% glass seal has the fewest total number of AE events recorded during testing. These two facts suggest that the 50% glass seal performs best when sealing ceramic to metal, which is opposite the results for sealing ceramic to ceramic.

The test specimens have also been observed after AE analysis is complete. Once testing is completed, the seal remains firmly attached to the ceramic disk. On the other hand, the seal is completely detached from the metal disk. From this, it is assumed that the seal material and the metal disk have the weakest interface.

4.2 Glass Characterization Results

As was mentioned in Section 3, high fidelity FEA results require good material properties. The stress/strain tests are used to find Young's Modulus for the glass specimens at room temperature, 200°C, and 350°C. The results of stress vs. strain are shown in Figures 22-23 for room temperature, 200°C, and 350°C respectively. The graphs have been modified to compensate for settling and slipping of the extensometer during testing.

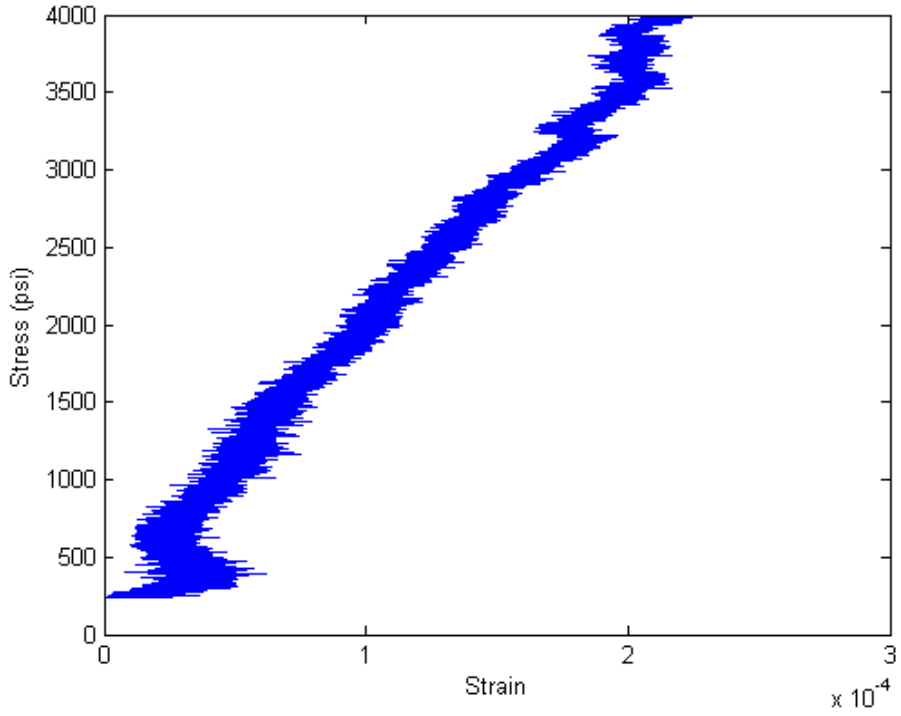

Figure 22: Stress/strain curve for glass specimen at 23°C

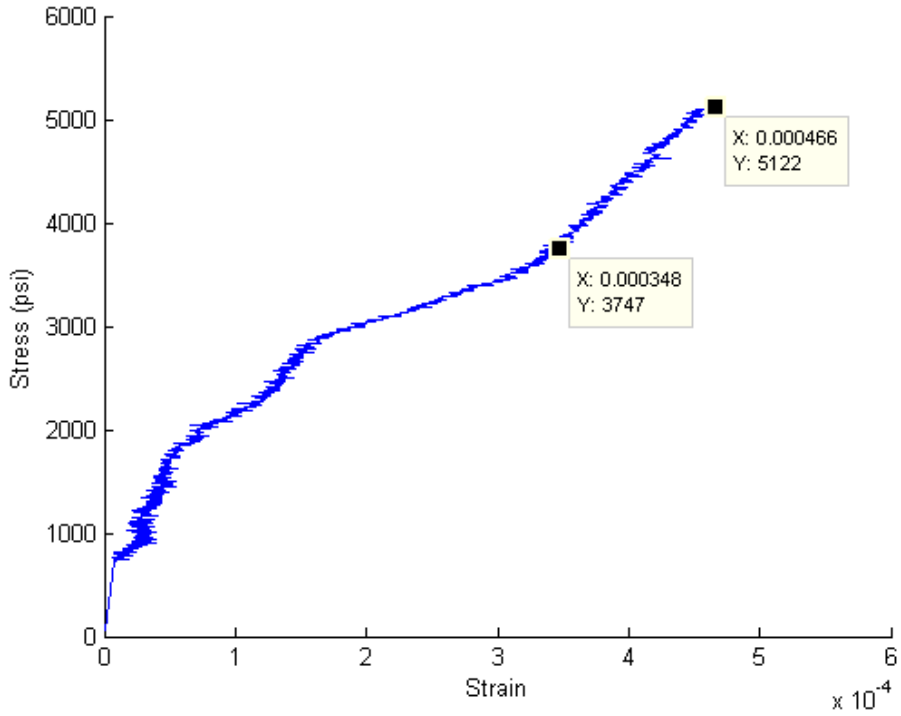

Figure 23: Stress/strain curve for glass specimen at 350°C

The stress/strain curves give Young's Modulus for the glass at two different temperatures. The results are shown in the Table 6. It is seen that Young's Modulus varies slightly with temperature. The glass material properties found in this glass characterization can now be put into the glass-Zirconia composite seal material model in the FEA simulation. The published value of Young's Modulus is about 40 GPa from the manufacturer [18].

Table 5: Young's Modulus for glass at 23°C and 350°C

Temperature (°C)	23	350
Young's Modulus, E (GPa)	90	80

The glass characterization creep tests resulted in two graphs of strain vs. time. The results are shown in Figures 24-25. Figure 24 is the creep results for the glass specimen at 200°C. Figure 25 is the creep test results for the glass specimen at 500°C. The experimental results in Figures 24-25 are noisy because of extensometer drift that occurs over time.

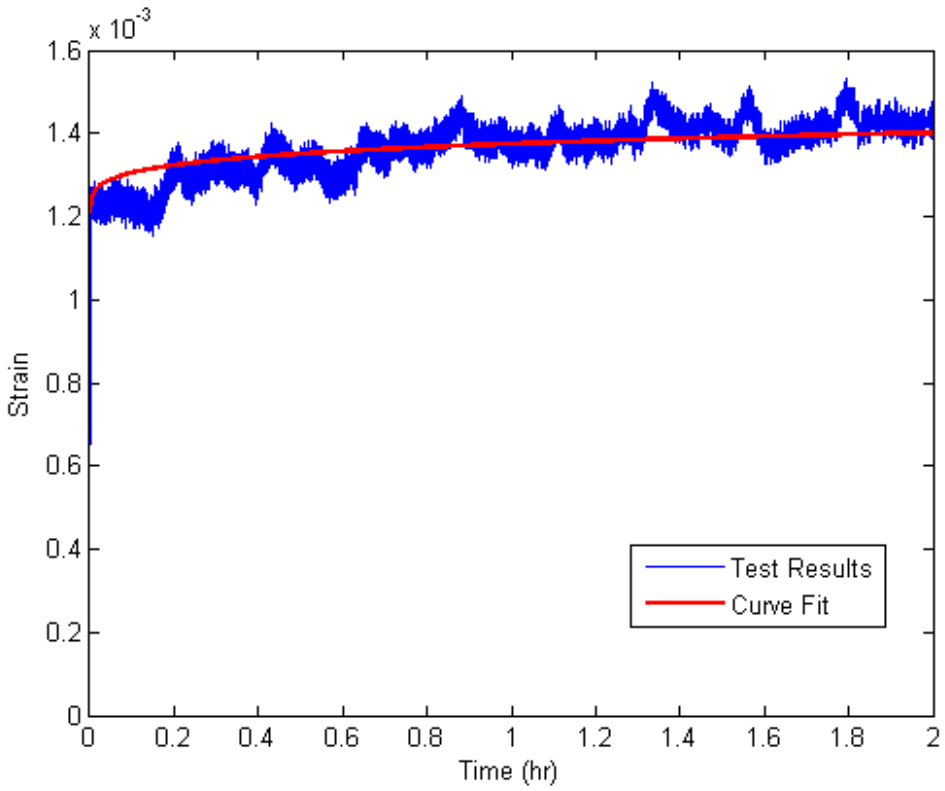

Figure 24: Strain vs. time for 200°C and 550 psi with creep curve fit overlay

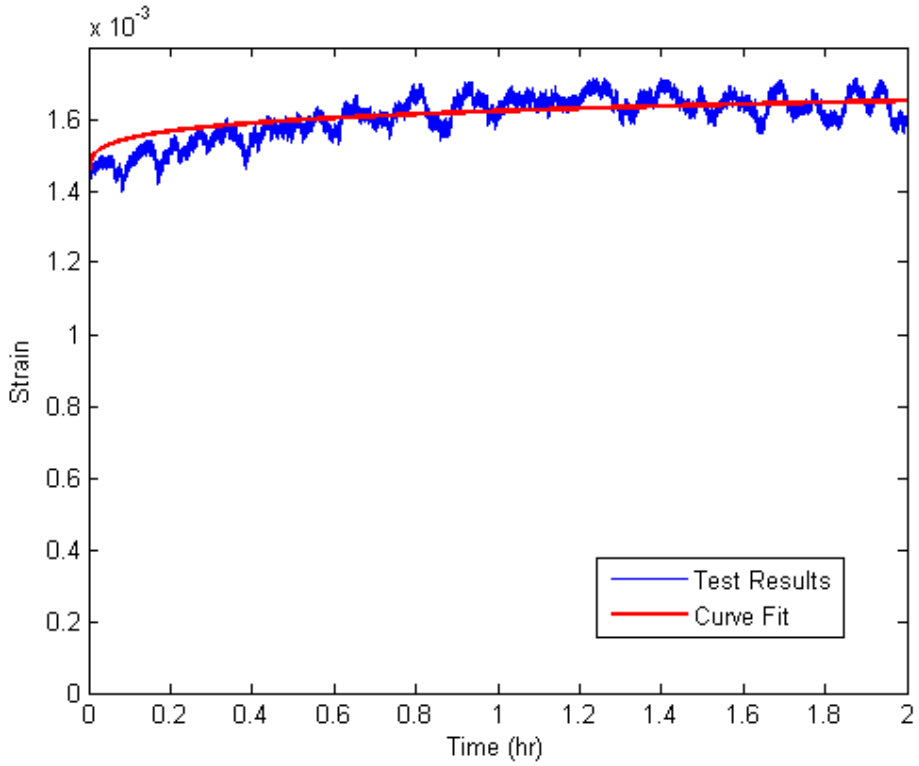

Figure 25: Strain vs. time for 500°C and 550 psi with creep curve fit overlay

A curve fit is used to determine the creep properties for the glass-Zirconia composite FEA material model. Since the experimental data is in strain vs. time, Equation 1 is integrated to obtain:

$$\varepsilon_{cr} = c_1 \sigma^{c_2} t^{c_3} e^{c_4/T} \quad (2)$$

The second constant, c2, is assumed to be 1.1 [19] since there are no stress variations between the creep tests to determine the stress dependence of creep. The c2 term is constant throughout all the tests, since stress is constant. The third constant, c3, is varied to meet the general shape of the strain vs. time graphs. Since c3 is time raised to an exponent, changing c3 changes the curvature of the curve fit. Making c3 more negative makes the curve flatter (strain does not change much with time), while making c3 less negative causes the strain to increase more quickly in time. The fourth constant, c4, is varied to change the temperature dependence of creep. In the curve fitting process, c4 changed the relationship between the two creep test results since the only change between the two is temperature. The c4 term in the equation is constant for each test, but it is a different constant because the temperatures of the two tests are different. Once the shape of the curves is determined by c3 and the relationship between the two curves is determined by c4, the proportional term, c1, is adjusted until the amplitudes of the creep results is correct. The c1 term is constant for all creep tests for the same material so it is the last term that is adjusted.

The creep constants determined from glass characterization are shown in Table 5.

Table 6: Creep constants found from glass characterization tests

c1	$3.8 \cdot 10^{-12}$
c2	1.1
c3	-0.83
c4	100

4.3 FEA Results from Ansys™

The FEA simulation is run as described in Section 3.5. The simulation takes about 30 minutes to run through the three load steps, because of nonlinearities in the seal material model. Once the simulation is completed, the stresses in the test specimen are analyzed in various ways. Graphs of stress vs. time are used to describe how stresses change at a particular node throughout the entire simulation. Stress contour plots are used to visually show the stress distribution for the entire specimen at a specific time. Videos can be used to combine the two by visually showing the stress contours for the entire specimen as it changes throughout the simulation. Figures 27-30 show the stress vs. time graphs for the three normal stresses and three shear stresses: σ_x, σ_y, σ_z, and τ_{xy}, respectively. The x, y, z coordinates were defined Figure 13. The stress plots are taken from the node closest to the center of the disk at the seal/metal interface. The location of this node is shown in Figure 26.

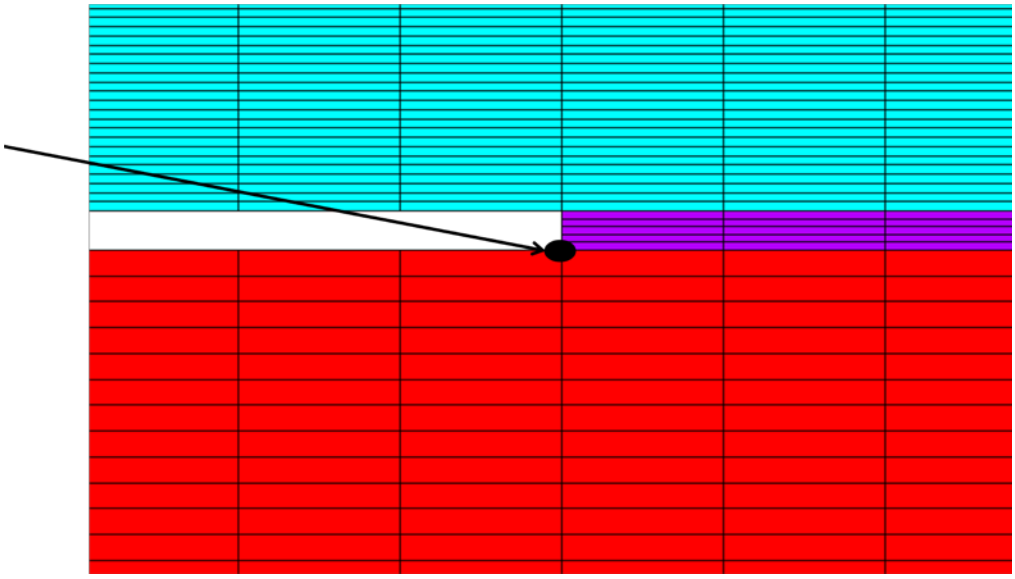

Figure 26: Location of the node used for stress vs. time analysis

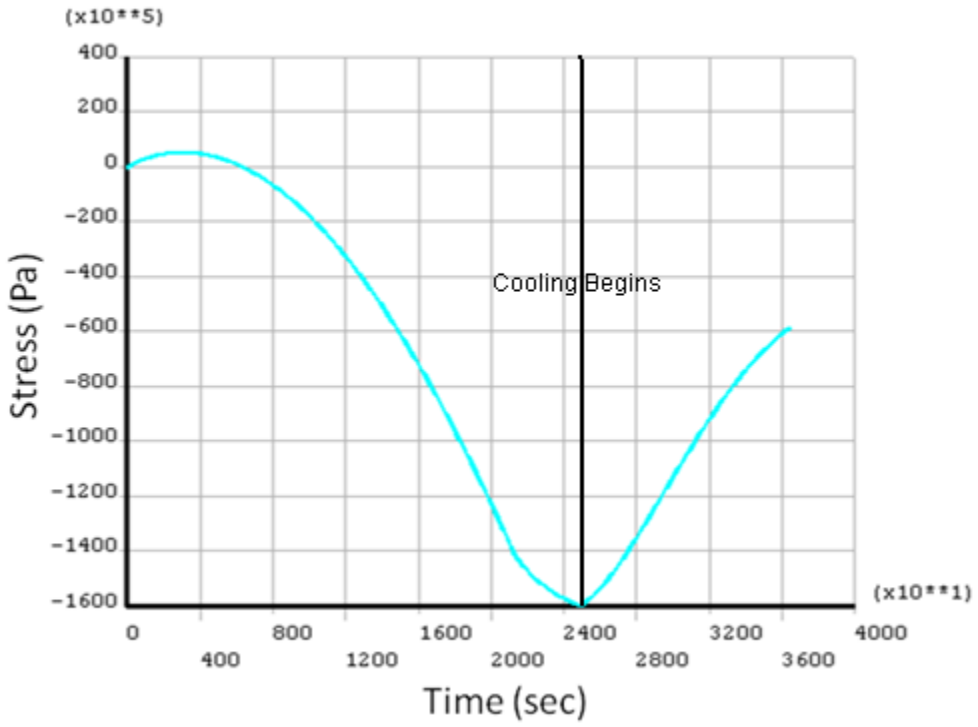

Figure 27: Normal stress in the direction radial from the center of the disk, σ_x

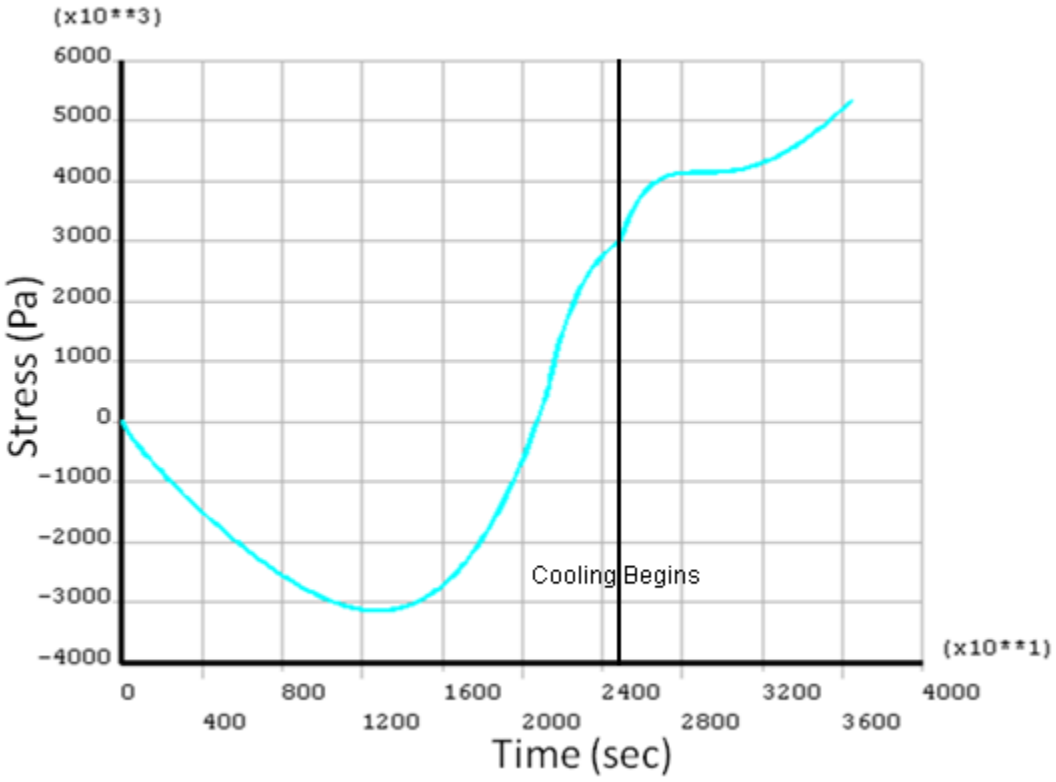

Figure 28: Normal stress in the direction of disk thickness, σ_y

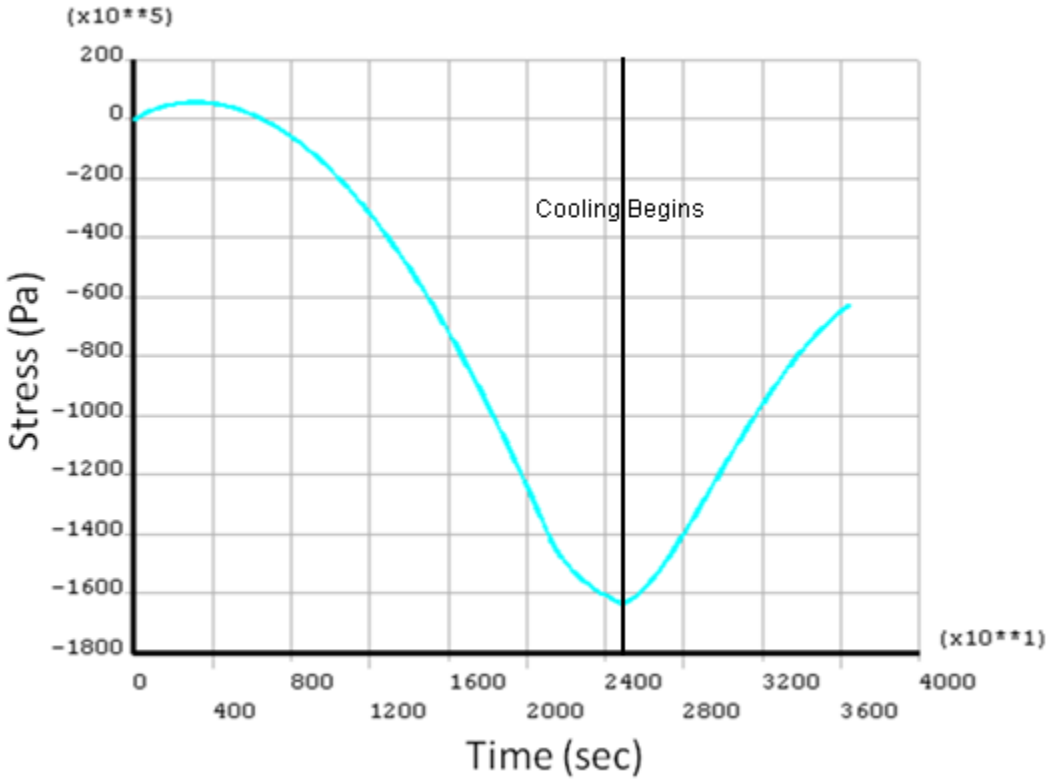

Figure 29: Normal stress in the direction tangential to the disk, σ_z

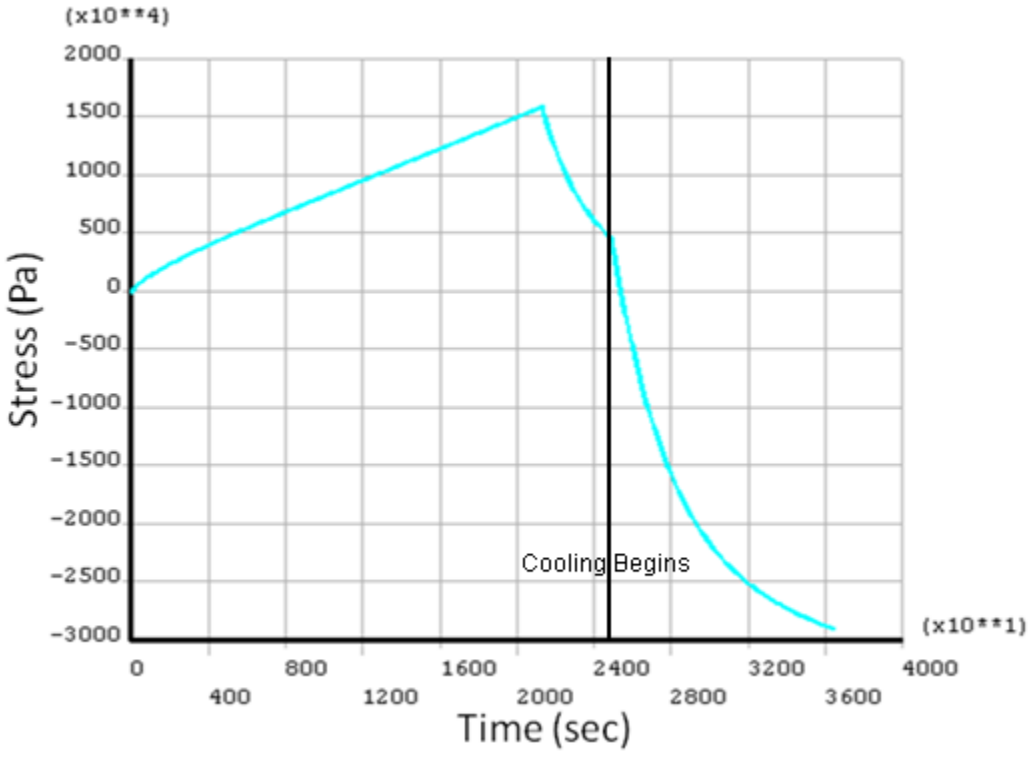

Figure 30: Shear stress between the radial and thickness directions, τ_{xy}

Since the expected cause of failure is separation between the seal and the crofer disk, stress in the thickness direction, σ_y, is expected to cause the failure. Based on the plot, the stress is compressive during heating. Once the holding stage begins, however, the stress becomes tensile. This occurs because bending due to thermal expansion mismatches is the main cause of stress. During heating, the bending causes compression at the seal/crofer interface. Because of creep properties, the glass seal settles during the high temperature hold period. Once cooling begins, the specimen bends in the opposite direction as before, causing tension at the seal crofer interface. The stress in the thickness direction becomes increasingly tensile throughout the cooling of the specimen, which is the likely cause of separation of the seal from the crofer. Under the assumption that the seals fail within the range of t_{cr} found from AE analysis, the strength of the bond between the seal and crofer is only between 0.003 GPa and 0.004 GPa. This seems logical since the temperature is still well above the glass annealing point when failure occurs, so the interface strength is much lower than the tensile strength below the annealing point. Any stress in the FEA simulation after separation is invalid, because Ansys™ assumes the model remains intact throughout the entire simulation.

5. Conclusions and Future Work

For sealing ceramic to ceramic, all three seals performed well, which is expected because there is no thermal expansion mismatch between the materials being sealed together. Based on the fact that there are only 7 AE events over a 20 hour time period (about 1 event every 3 hours), the 100% glass seal is assumed to be best suited for sealing ScSZ to ScSZ. The 100% glass seal is a viable seal material for sealing ceramic materials to like ceramic materials.

The results for sealing ceramic to metal are not as clear cut. Based on the critical time, t_{cr}, the 50% glass - 50% Zirconia seal is best suited for sealing crofer to ScSZ. However, all three seal materials exhibit large amounts of AE activity during the beginning of the cooling stage, which corresponds to material failure during SOFC shut-down. Further testing is required for more seal materials to find a viable solution to this problem. Based on the results of the AE analysis, some form of glass reinforced with ceramic is a likely solution to the SOFC sealing issue. The ceramic reinforced glass seals are much stiffer than 100% glass seals, making the seals less prone to failure.

The FEA simulation results seem to validate the findings of the AE analysis. Tensile stresses at the interface between the seal material and the crofer disk cause for the separation of the two materials during cooling. The tensile stress increases continuously throughout the cooling stage until the bond between the materials is broken. For all test specimens, the majority of the AE activity occurs during the cooling stage. This explains the incapability of SOFCs to be used multiple times. As stated before, SOFCs have been used efficiently for one use. With each subsequent cool-down and startup, the SOFC becomes significantly less efficient. Seal interface degradation is the most likely cause of this problem.

Further investigation is required to verify these findings. More test specimens of the same materials should be tested using the same AE analysis techniques. These experiments would provide results that could verify the repeatability of the data. Further glass characterizations need to be

performed to validate the accuracy of the creep model and stress/strain data of glass. Also, glass reinforced with ceramic could be tested for creep and stress/strain properties. Finally, FEA simulations could be run for each specimen tested in the AE experiments.

References

[1] Taniguchi, S., Kadowaki, M., Yasuo, T., Akiyama, Y., Miyake, Y., & Nishio, K. (1999). Improvement of thermal cycle characteristics of a planar-type solid oxide fuel cell by using ceramic fiber as sealing material. *Journal of Power Sources. 90*, 163-169.

[2] Ronan, P. (2007, October 16). *Solid Oxide Fuel Cells*. Retrieved June 2007, from Wikipedia: http://en.wikipedia.org/wiki/Image:Solid_oxide_fuel_cell.svg

[3] Alanne, K., Saari, A., Ugursal, V. I., & Good, J. (2005). The financial viability of an SOFC cogeneration system in single-family dwellings. *Journal of Power Sources*, *158*, 403-416.

[4] Badwal, S. P. S. (2001, June 8). Stability of solid oxide fuel cell components. *Solid State Ionics*, *143*, Retrieved October 2, 2006, http://www.sciencedirect.com

[5] Wen, T. L., Wang, D., Chen, M., Tu, H., Lu, Z., Zhang, Z., Nie, H. & Huang, W. (2002). Material research for planar SOFC stack. *Solid Stated Ionics*. *148*, 513-519.

[6] Bram, M. (2004).Deformation behavior and leakage tests of alternate sealing materials for SOFC stacks. *Journal of Power Sources*. *138*, 111-119.

[7] Ohara, S., Mukai, K., Fukui, T., Sakaki, Y., Hattori, M. & Esaki, Y. (2001). A new sealant material for solid oxide fuel cells using glass-ceramic. *Journal of the Ceramic Society of Japan*. *109*, 186-190.

[8] Chou, Y. S. & Stevenson, J. W. (2002).Thermal cycling and degradation mechanisms of compressive mica- based seals for solid oxide fuel cells. *Journal of Power Sources*. *112(2),* 376-383.

[9] Chou, Y. S., Stevenson, J. W., & Chick, L. A. (2002). Ultra-low leak rate of hybrid compressive mica seals for solid oxide fuel cells. *Journal of Power Sources. 112(1)*, 130-136.

[19] Chou, Y. S. & Stevenson, J. W. (2003). Phlogopite mica-based compressive seals for solid oxide fuel cells: effect of mica thickness. *Journal of Power Sources, 124(2)*, 473-478.

[11] Chou, Y. S. & Stevenson, J. W. (2003). Novel silver/mica multilayer compressive seals for solid-oxide fuel cells: The effect of thermal cycling and material degradation on leak behavior. *Journal of Materials Research, 18(9)*, 2243-2250.

[12] Chou, Y. S., Stevenson, J. W., & Chick, L. A. (2003). Novel compressive mica seals with metallic interlayers for solid oxide fuel cell applications. *Journal of the American Ceramic Society, 86(6)*, 1003-1007.

[13] Chou, Y. S. & Stevenson, J. W. (2003). Mid-term stability of novel mica-based compressive seals for solid oxide fuel cells. *Journal of Power Sources, 115(2),* 274-278.

[14] Chou, Y. S. & Stevenson, J. W. (2004). Novel infiltrated phlogopite mica compressive seals for solid oxide fuel cells. *Journal of Power Sources, 135(1-2)*, 72-78

[15] Vallen-Systeme. (1997-2008). *Acoustic Emission Instrumentation*. Retrieved March 2007, from Vallen-Systeme: http://www.vallen.de/index.html

[16] ThyssenKrupp. (2006, December). *Crofer 22 APU*. Retrieved September 2007, from ThyssenKrupp: http://thyssenkruppvdm.de/_pdf/Crofer22APU_e.pdf

[17] Ansys™ 11.0 Documentation (2007). *Table 2.4 Implicit Creep Equations*.

[18] ESCO Products (2005). *PYREX® (Corning 7740)*.Retrieved April 2008, from ESCO Products: http://www.escoproducts.com/html/pyrex_r_.html

[19] Widjaja, S., Yip, T. H., & Limarga, A. M. (2001). Measurement of creep-induced localized residual stress in soda-lime glass using nano-indentation technique. *Materials Science & Engineering. A318,* 211-215.